Spin Injection into Organic Light-Emitting Devices with Ferromagnetic Cathode and Effects on Their Luminescence Properties

Eiji SHIKOH*, Akihiko FUJIWARA, Yasuo ANDO[1] and Terunobu MIYAZAKI[1]

School of Materials Science, Japan Advanced Institute of Science and Technology, 1-1 Asahidai, Nomi, Ishikawa 923-1292, Japan

[1] *Department of Applied Physics, Graduate School of Engineering, Tohoku University, Aoba-yama 6-6-05, Sendai 980-8579, Japan*

Abstract

We investigated the luminescence properties of organic light-emitting devices under an external magnetic field. Circularly polarized light was observed from the devices with an Fe cathode, whereas those with an Al cathode did not show such behavior. The degree of circular polarization on the device with an Fe cathode increased with increasing applied magnetic field and decreased with increasing emissive layer thickness. These phenomena can be well explained in terms of the recombination of spin-polarized electrons injected from a ferromagnetic cathode. Consequently, spin diffusion length in the emissive layer, tris-(8-hydroxyquinolinato)-aluminum was estimated to be less than 60 nm from the thickness dependence of the degree of circular polarization.

KEYWORDS: spin injection, organic light-emitting device, ferromagnetic cathode, tris-(8-hydroxyquinolinato)-aluminum, circular polarization

*E-mail address: shikoh@jaist.ac.jp

1. Introduction

In recent years, the research field of spintronics has attracted much attention,[1)] because of its potential application to next-generation electronic devices. Injection of spin-polarized carriers into magnets, semiconductors and superconductors and manipulation of those injected into these materials are hot topics in this field. Circularly polarized luminescence due to the recombination of spin-polarized carriers in a light-emitting diode (LED) is one of the promising phenomena from the viewpoints of both basic research and applications. This luminescence can be used not only for the source of an intelligent light but also for determining of the degree of spin polarization. The circularly polarized luminescence due to spin injection has been achieved using inorganic GaAs-based LEDs.[2-6)] In these studies, spin injection efficiency and spin diffusion length in inorganic LEDs were estimated to be on the order of a few percent and over a hundred nanometers at room temperature, respectively. As an organic LED (OLED)[7, 8)] is a good candidate for a thin, light and flexible full-colored display, the circularly polarized luminescence produced using the OLED could be applied to a much more intelligent display, such as a three-dimensional display device. In spite of these

merits, spin-dependent electroluminescence (EL) has not been fully explored because of technical problems. In OLEDs, ferromagnetic metals as spin injectors are not appropriate for a cathode because they have a relatively high work function, which results in low luminescence efficiency.[9, 10] To our knowledge, no clear evidence for spin injection has been observed in OLEDs with a ferromagnetic cathode thus far.[11-15]

In this paper, we report the fabrication and EL properties of OLEDs with Fe, Co, $Ni_{81}Fe_{19}$, and Al cathodes and the electrical conduction properties of OLEDs with Fe and Al cathodes. We discuss the clear discrepancy between the EL properties of devices with Fe and Al cathodes in terms of the spin-polarized luminescence effect.

2. Experimental Details

2.1. Sample preparation

Figure 1 shows the stacking structure of an OLED that has been optimized on our experiments: a glass-substrate / ITO (In_2O_3 + SnO_2 10 wt %, transparent anode; thickness, 40 nm) / TPD (*N*,*N*'-bis(3-methylphenyl)-*N*,*N*'-diphenylbenzidine; 45 nm) / Alq_3 (tris-(8-hydroxyquinolinato)-aluminum; *d*) / Al-O (aluminum-oxide, tunnel

barrier; 1.0 nm) / M (cathode; 20 nm) / Al (capping cathode; 120 nm). TPD (purity, 99%; Sigma-Aldrich Japan) and Alq_3 (>99%; Gelest) were used as a hole transport layer and an emissive layer, respectively. Emissive layer thickness *d* was changed from 30 to 65 nm. As a cathode M, ferromagnetic metals Fe, Co and $Ni_{81}Fe_{19}$ were used and a nonmagnetic metal Al was used for comparison. A thin aluminum-oxide (Al-O) layer as a tunnel barrier was inserted at the interface between the cathode M and the Alq_3 layer, which would result in effective spin-polarized electron injection from the ferromagnetic metal cathode into the Alq_3 layer[16, 17] and reduce unexpected interactions between them.[14, 18]

An ITO (5.0 × 20 mm^2 area) as an anode was deposited on a clean glass substrate using RF magnetron sputtering with a shadow mask. After pumping the vacuum chamber down to its base pressure of < 1.0×10^{-4} Pa, argon gas was introduced up to 0.50 Pa. The deposition was carried out at a nominal deposition rate of 0.5 nm/s without control of the substrate temperature. To form a luminescence area without unexpected conduction paths, an edge-covering layer of Al_2O_3 (thickness; 80 nm) with a 2 × 2 mm^2 window for luminescence at the center of ITO was formed using photolithography and

conventional RF magnetron sputtering. A TPD layer, an Alq_3 layer and an Al layer for making an Al-O tunnel barrier with a 20×5.0 mm^2 area including the luminescence area were formed on the sample substrate using sequential vacuum ($< 4.0 \times 10^{-4}$ Pa) vapor deposition. The deposition rates monitored by a quartz resonator were 0.20, 0.20 and 0.03 nm/s, respectively. The substrate temperature during the sequence of evaporation was kept at –2 ºC. After the Al deposition, the sample substrate was exposed to air in the vacuum chamber for 5 min in order to oxidize the Al layer. Finally, a cathode M and an Al layer for capping were deposited by electron beam deposition at respective deposition rates of 0.03 and 0.10 nm/s, with the substrate cooled at –2 ºC.

2.2. Measurement methods

The EL spectra of OLEDs in the absence of an applied magnetic field were measured using a high-sensitivity multichannel spectro-photodetector (Otsuka Electronics, MCPD-7000). The luminescence properties of each OLED were observed through the glass substrate (Fig. 1).

Figure 2 shows the measurement system used for determining luminescence

properties under an applied magnetic field. To detect a small difference in polarization, AC modulation measurement was performed. OLEDs were operated using a DC bias voltage and a sine wave modulation voltage (200 Hz, $\pm$ 0.1 V). σ^+ and σ^- indicate the right and left circularly polarized light emitted from samples, respectively. σ^+ and σ^- were respectively transformed to mutually orthogonal linear polarized light, σ^+' and σ^-', by using a quarter-wave plate (Sigma Koki). They were separated by a polarizing beam splitter (Sigma Koki) and each divided light was detected by a silicon photodiode (Hamamatsu Photonics, S1337-66BR). $I_{\sigma+}$ and $I_{\sigma-}$ indicate the photocurrents on σ^+' and σ^-', respectively. The derivative of the total intensity of σ^+' and σ^-', $dI_{total}/dV = d(I_{\sigma+} + I_{\sigma-})/dV$, and the derivative of the difference intensity of σ^+' and σ^-', $d\Delta I/dV = d(I_{\sigma+} - I_{\sigma-})/dV$, were measured using a lock-in amplifier with a pulse generator (Seiko EG&G, 5210). Here, we assume that $I_{\sigma+}$ ($I_{\sigma-}$) is proportional to the intensity of σ^+' (σ^-'). The lock-in frequency and the time constant were 200 Hz and one second, respectively. The degree of circular polarization P is defined as

$$P = (I_{\sigma+} - I_{\sigma-})/(I_{\sigma+} + I_{\sigma-}) \times 100\ (\%) = \Delta I/I_{total} \times 100\ (\%). \qquad (1)$$

By considering the monotonous relation between the EL intensity and its driving bias

voltage, it is reasonable to replace intensities ΔI and I_{total} with derivative intensities $d\Delta I/dV$ and dI_{total}/dV, respectively. In addition, to reduce extrinsic error in data, such as the effect of dark current, derivative difference intensity $d\Delta I/dV$ is estimated by the difference that without applied magnetic fields (H = 0 Oe) as $d\Delta I(H)/dV$ - $d\Delta I(H$ = 0 Oe)/dV . Then P used in this work is expressed as

$$P = [d\Delta I(H)/dV - d\Delta I(H = 0\ \text{Oe})/dV\ ]/(\ dI_{total}/dV\ ) \times 100\ (\%). \qquad (2)$$

To avoid disturbance of circularly polarized light by magnetic fields, a magnetic field was applied parallel to the emitting light direction, namely, perpendicular to the ferromagnetic cathode film. The maximum magnetic field applied to samples was 2 T, produced using a couple of electromagnetic coils in this system. All measurements of luminescence properties were carried out at room temperature.

The electrical conduction properties of OLEDs were measured using a two-terminal method. Magnetic properties were measured using a SQUID magnetometer and the magnetic field was applied perpendicular to the substrate up to 5 T; this setup configuration corresponded to that for the measurements of electroluminescence under an applied magnetic field.

3. Results and Discussion

3.1. EL and conduction properties of various OLEDs

Figure 3 shows the EL spectra of various OLEDs with a cathode [(a) M = Al, (b) M = Fe, (c) M = $Ni_{81}Fe_{19}$ and (d) M = Co] in the absence of an applied magnetic field. The emissive layer thickness *d* and drive current density were 45 nm and 25.0 mA/cm^2, respectively. Each spectrum is normalized to have the same maximum intensity by the expansion rates indicated in the figure. The spectra and respective baselines are shifted for clarity. There was little difference in the peak wavelength among spectra and the peak position was almost consistent with typical previous reports.[19-22)] The luminescence intensity of the OLED with an Fe cathode was the strongest among those of three OLEDs with the ferromagnetic cathodes, even though it was weaker than that of the OLED with an Al cathode.

One reason for the difference in luminescence intensity is the difference in work function among the cathode metals.[9, 10)] The differences between the lowest unoccupied molecular orbital (LUMO) level of Alq_3 and the work functions of Al (4.2 eV), Fe (4.4

eV), Co (4.4 eV), and $Ni_{81}Fe_{19}$ (4.7 eV) are expected to be 1.2, 1.4, 1.4, and 1.7 eV, respectively. It is possible for a relation between the energy difference and suppression of EL intensity to exist. Imperfection at the interface between the cathode and emissive layer[14, 18, 23-25] might also cause a decrease in EL intensity as a minor effect. The ferromagnetic metal atoms can diffuse into the emissive layer through the defects of the thin Al-O layer during the deposition, and act as quenching centers by themselves and/or in combination with Alq_3 molecules.

High spin polarization at the Fermi energy level of electrodes is favorable for effective spin injection. The reported spin polarizations of Fe (45 %), Co (42 %), and $Ni_{81}Fe_{19}$ (45 %) are almost the same,[26, 27] suggesting that these ferromagnetic metals are expected to behave similarly as spin injectors. Hereafter, the OLED with M = Fe was focused as an OLED with a ferromagnetic cathode because it showed the highest intensity among three OLEDs with a ferromagnetic cathode.

Figure 4 shows the electrical conduction properties of the OLEDs with M = Al (closed circles) and M = Fe (open circles). The regions below and above the slope change at a voltage V_{th}, corresponding to nonemissive and emissive states,

respectively.[20] Here, the threshold voltage V_{th} can be defined as the crossing point of the fitting line for both states and is pointed out by an arrow.[20] The V_{th} of the OLED with M = Al is approximately 6.5 V, which is consistent with previous reports.[9, 10, 22] In the case of the OLED with M = Fe, V_{th} is approximately 10 V, which is higher than that of the OLED with M = Al. This could be due to the relatively high work function of Fe.

3.2. Luminescence properties of OLEDs under applied magnetic field

Figure 5 shows the relationship between electrical conduction and the derivative of PD current dI/dV for (a) an OLED with M = Al and (b) that with M = Fe in the absence of an applied magnetic field. In both figures, triangles indicate current density and closed and open circles correspond to the derivatives of $I_{\sigma+}$ and $I_{\sigma-}$, respectively. Each dotted line indicates the V_{th} of the OLED. In Fig. 5(b), dI/dV levels out around 6 nA/V up to 26 V, in spite of the emissive state. This means that those values originate from the dark current of the PD. To detect emission in terms of $dI_{\sigma+}/dV$ and $dI_{\sigma-}/dV$, measurements were performed at a drive voltage of 31 V. In the case of the OLED with M = Al in Fig. 5(a), the luminescence was detected using a relatively low applied

voltage of 23 V.

Figure 6 shows (a) the degree of circular polarization *P* from the OLEDs with M = Al, (b) that from the OLEDs with M = Fe and (c) the magnetization curve of the OLED with M = Fe, under magnetic field applied perpendicular to the OLED emissive plane. A few data for each OLED have been plotted, which are shown by different symbols. The drive voltage was fixed at 23 V for the OLEDs with M = Al and at 31 V for those with M = Fe, respectively. The *P* for M = Fe linearly increased with increasing external applied magnetic field and no hysteresis character was observed. It was also confirmed that no circular polarization was observed in the absence of an applied magnetic field. These behaviors were observed on 60% of the samples fabricated in this study. Note that the change in device current under an applied magnetic field is much smaller than that in *P* as a function of magnetic field. On the other hand, OLEDs with M = Al showed no circular polarization. These results suggest that the magnetized cathode certainly causes the circular polarization. As shown in Fig. 6(c), the magnetization of Fe films increases almost linearly with increasing magnetic field, and does not saturate up to 2 T. The sharp rise at around 0 T can be attributed to the slight misalignment from the

film surface perpendicular to the direction of the magnetic field, and is not essential for the magnetization process. The linear change in *P* from OLEDs with M = Fe could be attributed to the magnetization process of the Fe film.

Figure 7(a) shows the *d*-dependence of EL intensities without an applied magnetic field, and Figs. 7(b) and 7(c) show the *d*-dependence of *P* at 1 T and that at 2 T, respectively. Closed and open circles indicate data for M = Al and those for M = Fe, respectively. Dotted lines are guides to the eyes. *P* was calculated between *d* = 40 and 58 nm, in which region the EL intensity was large enough to calculate *P*. In spite of the small deviation of EL intensity in this region, the *P* of the OLEDs with M = Fe drastically decreased with increasing *d*.

Circular polarization from OLEDs with an ferromagnetic cathode can originate not only from the recombination of spin-polarized electrons injected from a ferromagnetic cathode but also from 1) a magnetic circular dichroism (MCD) effect at the Fe film surface, 2) an interference effect with the MCD effect and 3) a spin polarization at the Alq_3 layer. In the first case, if *P* were only due to the MCD effect of Fe, it should not depend on *d*. To check this effect, we measured photoluminescence for Alq_3 films on Fe

and Al films under an applied magnetic field of ± 0.35 T and no clear circular polarization was observed within experimental error. In the second case, the marked decrease in *P* in the narrow *d*-region between 40 and 58 nm cannot be explained. In the last case, circular polarization in EL must be observed similarly from OLEDs with nonmagnetic cathodes. On the basis of these reasons, it is reasonable that the origin of circularly polarized EL is attributed mainly to the recombination of spin-polarized electrons injected from a ferromagnetic cathode and that the decrease in *P* with increasing *d* is due to the spin diffusion of electrons in Alq_3. The yield of 60% and the low signal-to-noise ratio on data from devices with M = Fe might be due to the lowering of spin injection efficiency caused by the imperfection of the Al-O tunnel barrier.[14, 18)] The fact that *P* disappears at around *d* = 55 nm in Fig. 7 naively suggests that the spin diffusion length of Alq_3 film at room temperature is less than 60 nm. A value of similar order, 45 nm, at 11 K was reported for another experimental method.[28)]

In general, the spin-orbit interaction plays as an important role in circularly polarized luminescence and that of organic molecules is much smaller than that of inorganic GaAs-based semiconductors.[29)] This might be the reason for the small observed *P*. To

clarify the mechanism of circularly polarized luminescence from the Alq_3 layer, further investigation should be carried out. Experiments on other emissive molecules that have different energy states and/or spin states are one of the most important issues. Polarized-spin injection from a saturated ferromagnetic electrode is also an interesting subject of investigation. This phenomenon can be realized by applying intense magnetic fields in the same configuration as in this work, or by observing the luminescence from the edge (side) of OLEDs under magnetic fields parallel to the substrates.

4. Conclusions

We investigated the EL and electrical conduction properties of OLEDs with a ferromagnetic cathode. As a ferromagnetic cathode, Fe, Co and $Ni_{81}Fe_{19}$ were used and the OLED with an Fe cathode showed the highest intensity among the three OLEDs with a ferromagnetic cathode. When an external magnetic field was applied to the OLEDs with an Fe cathode, circular polarized EL was observed. The degree of circular polarization increased with increasing applied magnetic field and decreased with increasing emissive layer thickness. These suggested that the observed circular

polarization mainly originates from the spin injection from the Fe cathode into the Alq_3 layer. From the thickness dependence of the degree of circular polarization, spin diffusion length in the Alq_3 layer was estimated to be less than 60 nm.

Acknowledgement

This study was supported by a JSPS Research Fellowship for Young Scientists, a Grant for Basic Science Project from Sumitomo Foundation, a Grant-in-Aid for Scientific Research (Encouragement for Young Scientists (B) No. 17760009) from the Ministry of Education, Culture, Sports, Science and Technology, and a Grant (2004IT093) from NEDO.

References

1) S. A. Wolf, D. D. Awschalom, R. A. Buhrman, J. M. Daughton, S. von Molnár, M. L. Roukes, A. Y. Chtchelkanova and D. M. Treger: Science **294** (2001) 1488.

2) R. Fiederling, M. Keim, G. Reuscher, W. Ossau, G. Schmidt, A. Waag and L. W. Molenkamp: Nature **402** (1999) 787.

3) Y. Ohno, D. K. Young, B. Beschoten, F. Matsukura, H. Ohno and D. D. Awschalom: Nature **402** (1999) 790.

4) B. T. Jonker, Y. D. Park, B. R. Bennett, H. D. Cheong, G. Kioseoglou and A. Petrou: Phys. Rev. B **62** (2000) 8180.

5) H. J. Zhu, M. Ramsteiner, H. Kostial, M. Wassermeier, H.–P. Schönherr and K. H. Ploog: Phys. Rev. Lett. **87** (2001) 016601.

6) T. Manago and H. Akinaga: Appl. Phys. Lett. **81** (2002) 694.

7) C. W. Tang and S. A. VanSlyke: Appl. Phys. Lett. **51** (1987) 913.

8) J. Kalinowski: J. Phys. D **32** (1999) R179.

9) M. Stössel, J. Staudigel, F. Steuber, J. Simmerer and A. Winnacker: Appl. Phys. A **68**

(1999) 387.

10) M. Stößel, J. Staudigel, F. Steuber, J. Blässing, J. Simmerer, A. Winnacker, H. Neuner, D. Metzdorf, H.–H. Johannes and W. Kowalsky: Synth. Met. **111-112** (2000) 19.

11) A. H. Davis and K. Bussmann: J. Appl. Phys. **93** (2003) 7358.

12) E. Arisi, I. Bergenti, V. Dediu, M. A. Loi, M. Muccini, M. Murgia, G. Ruani, C. Taliani and R. Zamboni: J. Appl. Phys. **93** (2003) 7682.

13) A. H. Davis and K. Bussmann: J. Vac. Sci. Technol. A **22** (2004) 1885.

14) E. Shikoh, Y. Ando and T. Miyazaki: J. Magn. Magn. Mater. **272-276** (2004) 1921.

15) G. Salis, S. F. Alvarado, M. Tschudy, T. Brunschwiler and R. Allenspach: Phys. Rev. B **70** (2004) 085203.

16) G. Schmidt, D Ferrand, L. W. Molenkamp, A. T. Filip and B. J. van Wees: Phys. Rev. B **62** (2000) R4790.

17) E. I. Rashba: Phys. Rev. B **62** (2000) R16267.

18) E. Shikoh, Y. Ando and T. Miyazaki: J. Appl. Phys. **97** (2005) 10D501.

19) C. W. Tang, S. A. VanSlyke and C. H. Chen: J. Appl. Phys. **65** (1989) 3610.

20) P. E. Burrows, Z. Shen, V. Bulovic, D. M. McCarty, S. R. Forrest, J. A. Cronin and M. E. Thompson: J. Appl. Phys. **79** (1996) 7991.

21) Z. Shen, P. E. Burrows, V. Bulovic, D. M. McCarty, M. E. Thompson and S. R. Forrest: Jpn. J. Appl. Phys. **35** (1996) L401.

22) S. K. Saha, Y. K. Su and F. S. Juang: IEEE. J. Quantum Electron. **37** (2001) 807.

23) M. Probst and R. Haight: Appl. Phys. Lett. **70** (1997) 1420.

24) M. B. Huang, K. McDonald, J. C. Keay, Y. Q. Wang, S. J. Rosenthal, R. A. Weller and L. C. Feldman: Appl. Phys. Lett. **73** (1998) 2914.

25) A. Curioni and W. Andreoni: J. Am. Chem. Soc. **121** (1999) 8216.

26) D. J. Monsma and S. S. P. Parkin: Appl. Phys. Lett. **77** (2000) 720.

27) D. J. Monsma and S. S. P. Parkin: Appl. Phys. Lett. **77** (2000) 883.

28) Z. H. Xiong, D. Wu, Z. V. Vardeny and J. Shi: Nature **427** (2004) 821.

29) F. Meier and B. P. Zakharchenya: *Optical Orientation*, *Modern Problems in Condensed Matter Sciences* (North-Holland, Amsterdam, 1984) Vol. 8.

Figure captions

Fig. 1. Stacking structure of OLED that has been optimized in our experiments. M = Fe, Co, $Ni_{81}Fe_{19}$ or Al. Numerical values show the thickness of each layer.

Fig. 2. Measurement system for determining luminescence properties under applied magnetic field. σ^+ and σ^- indicate the right and left circularly polarized light, respectively.

Fig. 3. EL spectra of various OLEDs with cathode M when applied current density is 25.0 mA/cm^2; (a) M = Al, (b) M = Fe, (c) M = $Ni_{81}Fe_{19}$, and (d) M = Co. Each spectrum is normalized to have the same intensity by the expansion rates indicated in this figure. The spectra and respective baselines are shifted for clarity.

Fig. 4. Electrical conduction properties of OLEDs with M = Al (closed circles) and M = Fe (open circles). Dashed and solid lines show the fitting results for the nonemissive

and emissive states, respectively, by assuming a linear relation in logarithmic plots. Arrows indicate V_{th} (the cross point of two lines) for respective OLEDs.

Fig. 5. Relationship between electrical conduction and derivative of PD current *dI*/*dV* for (a) OLED with M = Al and (b) that with M = Fe in absence of applied magnetic field. Triangles indicate applied current density and closed and open circles correspond to the derivatives of $I_{\sigma+}$ and $I_{\sigma-}$, respectively.

Fig. 6. Degree of circular polarization *P* from OLEDs (a) with M = Al, (b) that from OLEDs with M = Fe and (c) magnetization curve of OLED with M = Fe. An external magnetic field is applied perpendicular to the OLED film plane.

Fig. 7. (a) Emissive layer thickness *d* dependence of EL intensities without applied magnetic field, (b) *d* dependence of degree of circular polarization *P* from OLEDs at 1 T and (c) that at 2 T. Closed and open circles indicate data for M = Al and M = Fe, respectively.

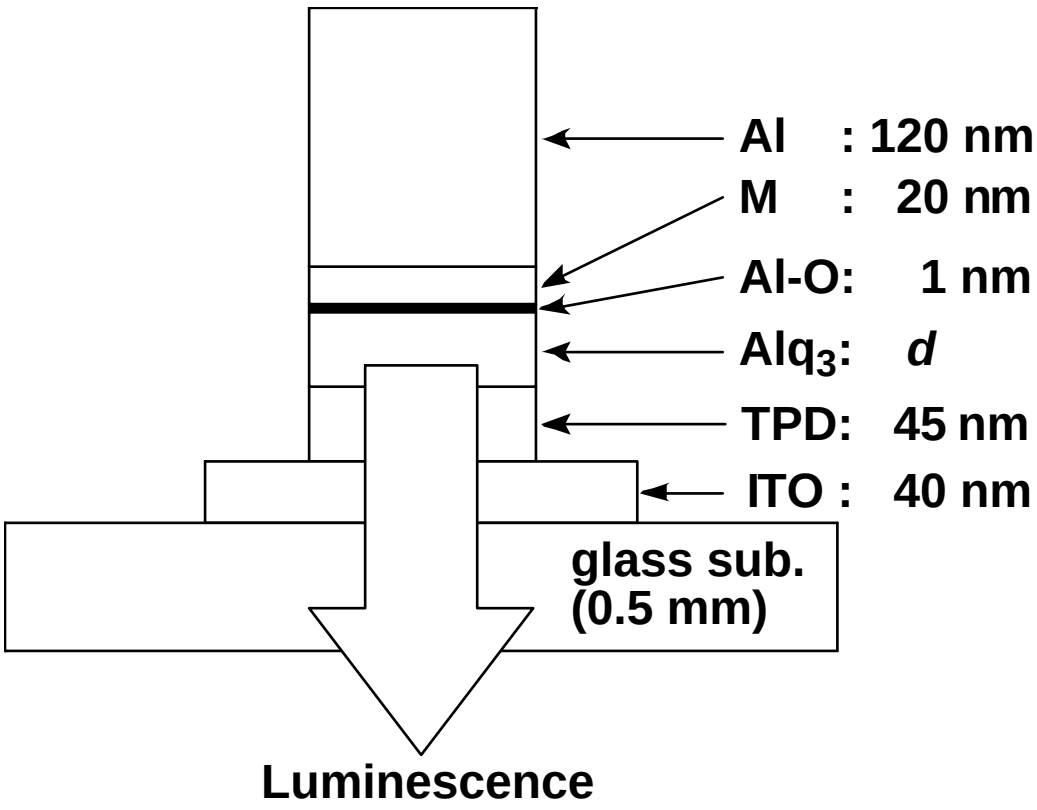

Fig. 1.

Eiji SHIKOH et al.

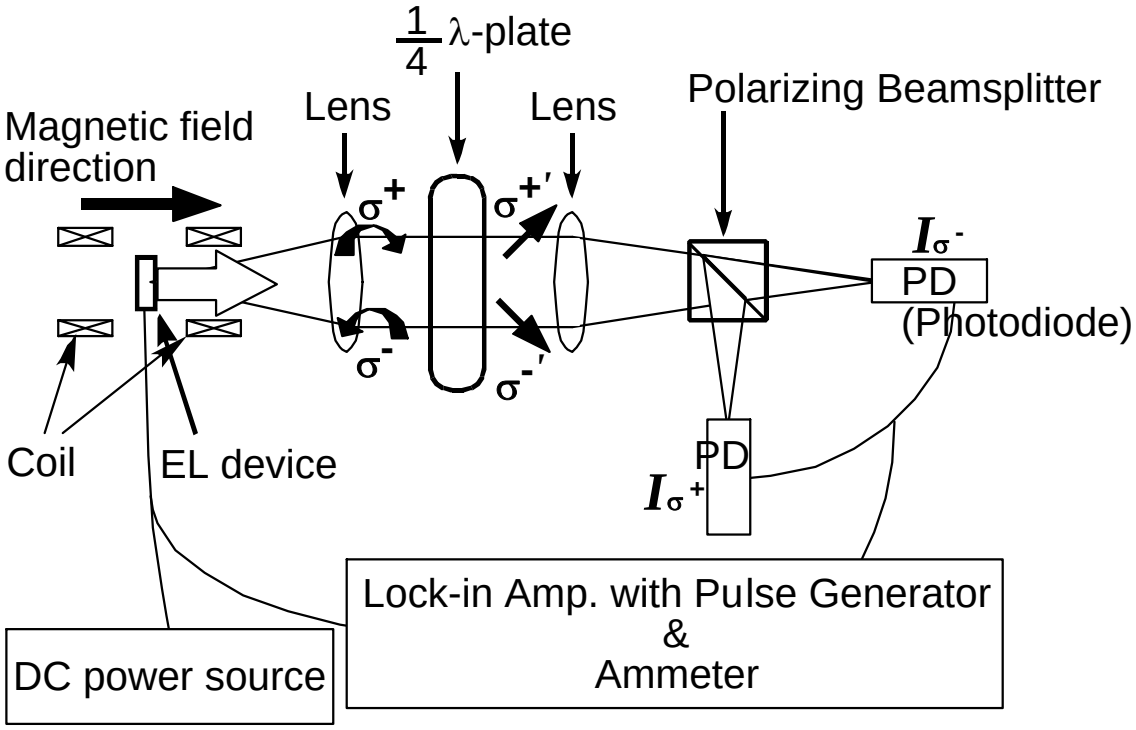

Fig. 2.

Eiji SHIKOH et al.

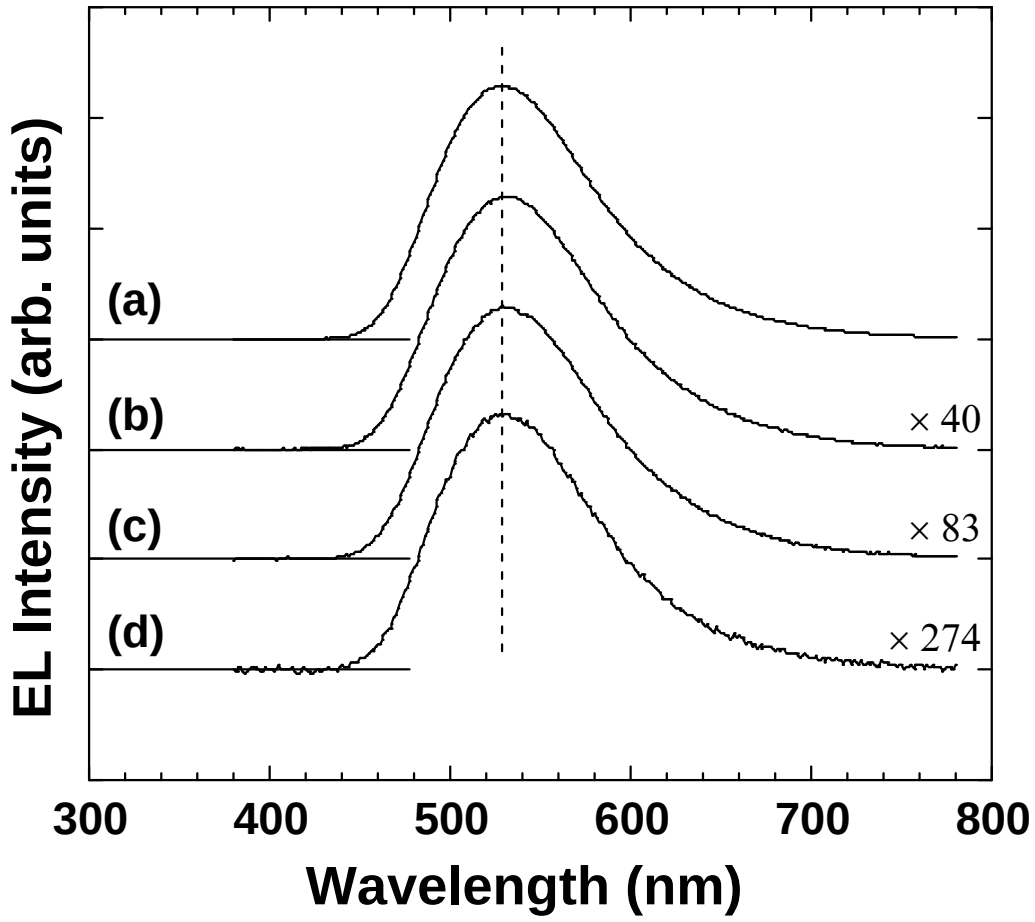

Fig. 3.

Eiji SHIKOH et al.

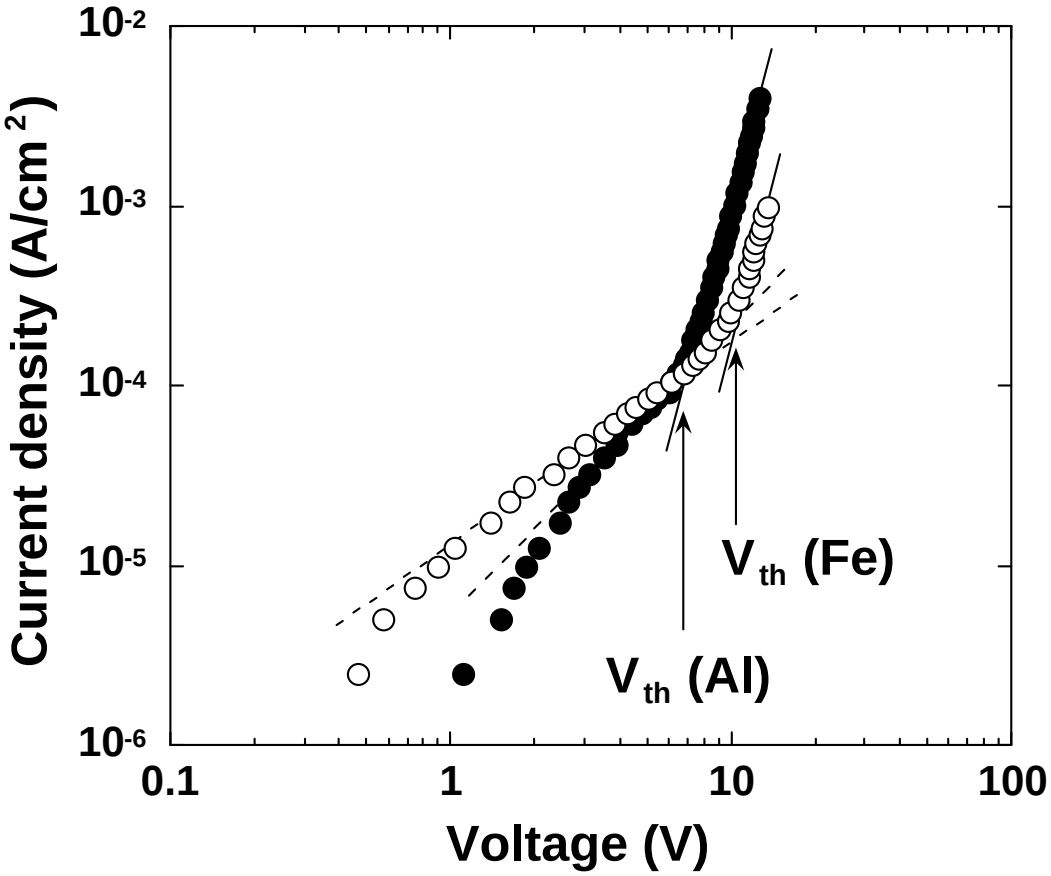

Fig. 4.

Eiji SHIKOH et al.

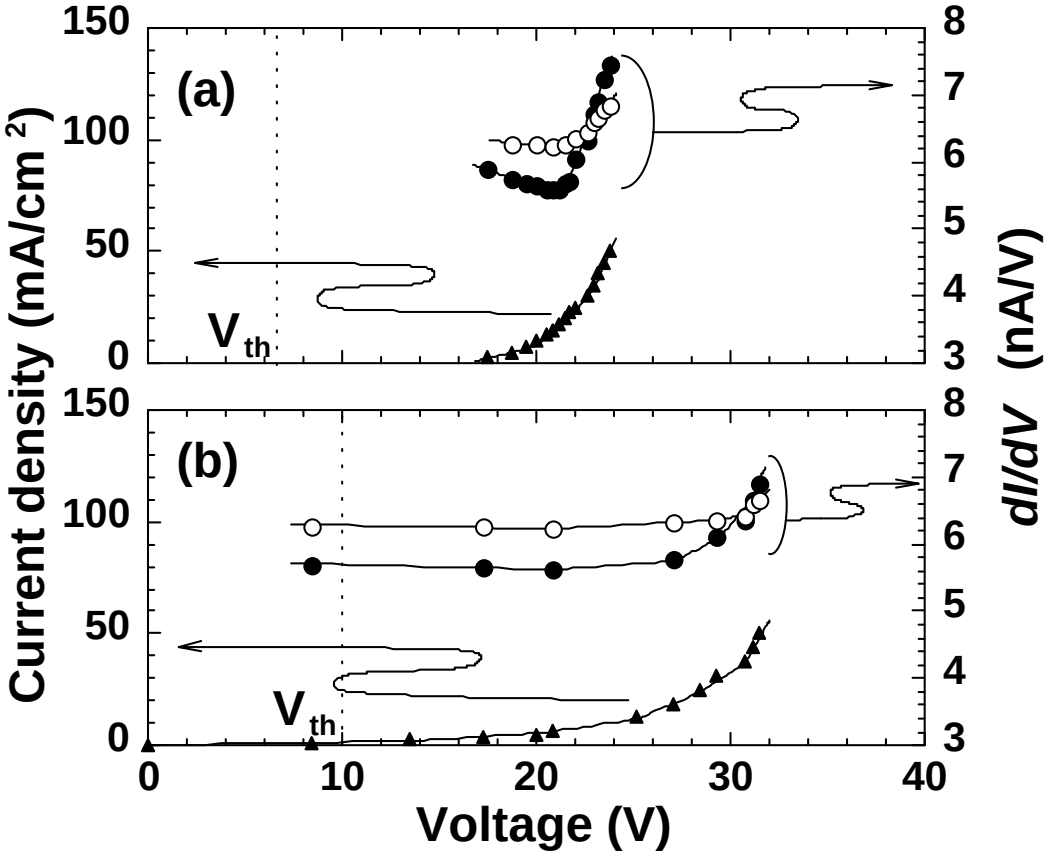

Fig. 5.

Eiji SHIKOH et al.

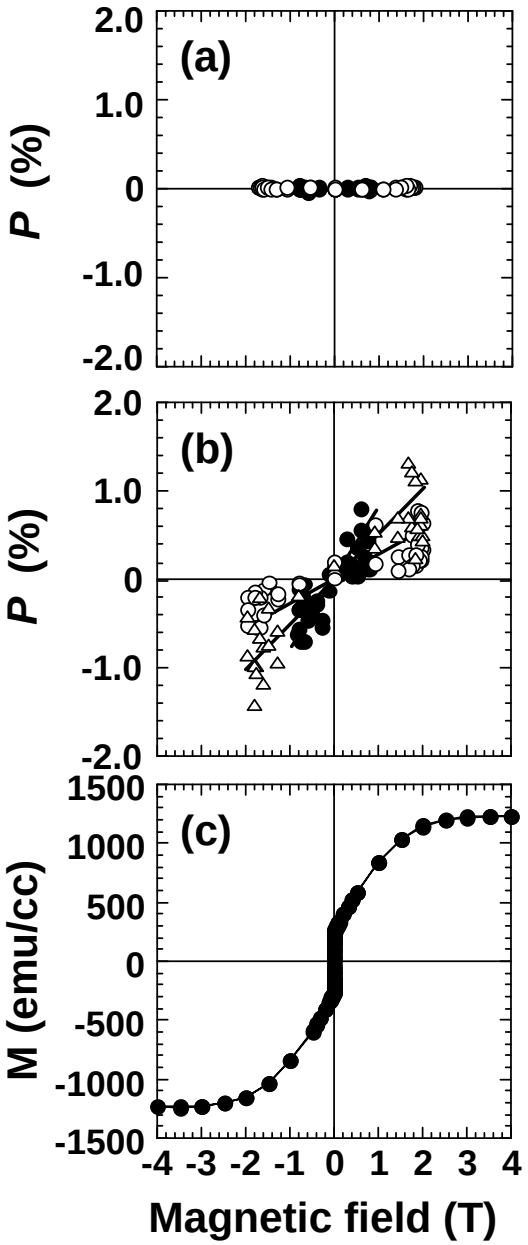

Fig. 6.

Eiji SHIKOH et al.

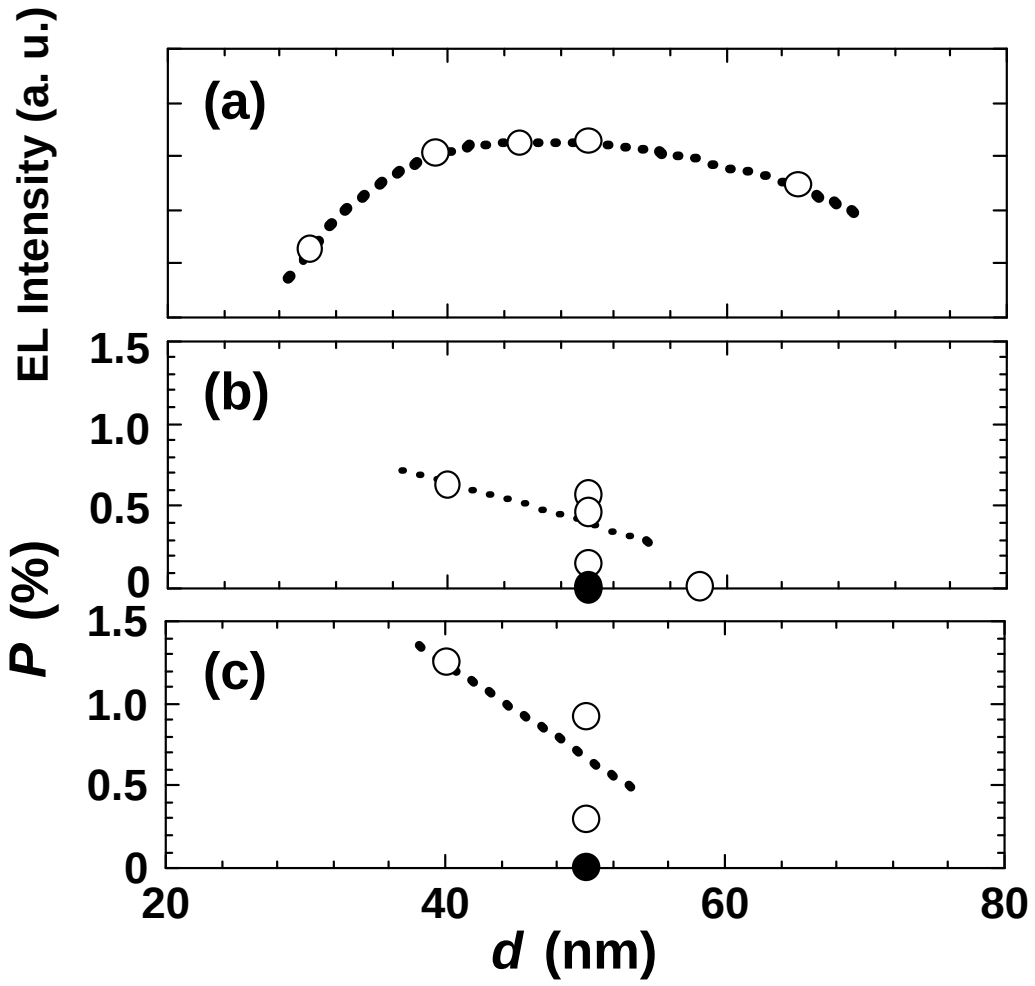

Fig. 7.

Eiji SHIKOH et al.